Beam instability at KEKB accelerator

K. Ohmi
KEK-IMSS

11 March 2000 : BIW@ESRF

1 Introduction

We face various beam instabilities in KEKB operation. These instabilities affect to limit of the luminosity. We focus beam instabilities caused by cloud of chraged particles in beam chamber.

- Ion instability in HER.
- Photoelectron instability in LER : multi-bunch mode.
- Photoelectron instability in LER : single-bunch mode.

We first review experiments, and discuss model and simulation.

2 Experiment

2.1 General

- Largest current stored so far after Belle roll-in is

  600 mA in LER and 435 mA in HER.

  Maximum luminosity is achived to be $1.09 \times 10^{33} cm^{-2} s^{-1}$ at around 500mA (LER) $\times$ 300mA (HER). Note that the max. was not achived at the largest currents.

- Fill pattern : 32/36/4 (trains/bunches in a train/bunch spacing in the unit of rf bucket)

  Coupled bunch instability(CBI) is completely suppressed by the bunch feedback system and large chromaticity. The chromaticity ξ_x/ξ_y is typically 5/8 in both rings.

  In LER the current is not limited by CBI. It is regulated to avoid the damage to the hardware.

  In HER beam loss occurs at the tail of a series of trains around 435 mA. CBI may be the cause of the beam loss. Detailed study have not done yet, because LER limits the collision performance.

- Vertical blow-up of beam size is observed in LER.

  The beam size as a function of beam current starts to increase at a threshold beam current and is almost doubled by 300 mA.

  The blow-up is one of the most serious problems limiting the luminosity of KEKB.

  Beam-beam interaction causes further beam blow up of LER, when the current exceed a threshold ($\sim 400mA$). Such blow up are not observed at a collision of a small number of bunches.

- Masks heating and longitudinal coupled bunch instability in LER.

  Vertical masks which reduces a detector background are heated up at high current.

  Longitudinal coupled bunch instability is caused by masks. The instability is very sensitive for the mask position. The longitudinal motion make worse the feed back gain.

  A bellows near IP heating also limits the maximum current.

2.2 Transverse coupled bunch instability in HER

2.2.1 Horizontal (HER)

- In an experiment trying to store high beam current (at chromatixity of $\xi_x = 5/\xi_y = 8$), bunch oscillation was measured by the Bunch Oscillation Recorder (single pass BPM + memory).

  BOR measures the transverse bunch position for 40 ms after turn-off the bunch feedback system.

- The beam conditions were,

  Fill pattern : 32/36/4

  Beam current: 435 mA

- Horizontal oscillation is much stronger than vertical in both rings.

- Gap between trains ($\sim 20 \times 2ns$) has alomost no effect.

  The correlation length (or range of the wake force) is longer than $40ns$.

- Growth time : 3.2ms (13ms in vertical at this experiment)

2.2.2 Vertical (HER)

- The beam conditions Vertical chromaticity : 3

  Fill pattern : 8/120/4

  Beam current: 240 mA

- Vertical oscillation are observed after cutting FB.

  Observed growth time : 57ms

- Relation between CBI mode and σ_y.

  Consistent with ion frequency in the beam potential.

2.3 Transverse coupled bunch instability in LER

2.3.1 Horizontal (LER)

- In an experiment trying to store high beam current (at chromatixity of $\xi_x = 5/\xi_y = 8$), bunch oscillation was measured by the Bunch Oscillation Recorder (single pass BPM + memory).

  BOR measures the transverse bunch position for 40 ms after turn-off the bunch feedback system.

  Fill pattern : 32/36/4

  Beam current : 600 mA

- Growth time : 1.3ms (not seen in vertical at this experiment)

- Gap between trains ($\sim 20 \times 2ns$) has an effect.

  The correlation length (or range of the wake force) is shorter than $40ns$.

2.3.2 Vertical (LER)

- The beam conditions

  Horizontal chromaticity : 1.56 Vertical chromaticity : 1.3, 3.3, 5.32

  Fill pattern : 4/60/6 240 bunch

  Beam current: 120 mA

- Vertical oscillation are observed after cutting FB for $\xi_y \leq 3.3$.

- Observed growth time :

  At $\xi_y = 3.3$, $\tau \sim 2.5ms$ beam loss $124mA \rightarrow 100mA$

  At $\xi_y = 1.3$, $\tau \sim 1ms$, beam current $100mA$.

2.4 Effect of chromaticity

Above two types of instabilities are bunch by bunch correlation of transverse dipole motion (coupled bunch instability).

Dipole oscillation is damped by the head-tail effect for an operation with a positive chromaticity (head-tail damping). The source of the head-tail effect is impedance of chamber wall. We can estimate it from current dependent tune shift.

The analysis is performed by solving eigenvalues and modes of linearized Vlasov equation (Yokoya's code).

2.4.1 HER

A measurement at a single bunch operation shows

$$\frac{d\nu_x}{dI} = -0.0010 mA^{-1} \quad (1)$$

$$\frac{d\nu_y}{dI} = -0.0043 mA^{-1} \quad (2)$$

The transverse wake forces are estimated to be

$$W_{1,x} = 0.96 \times 10^{18} z[V/Cm] \quad (3)$$

$$W_{1,y} = 4.0 \times 10^{18} z[V/Cm]. \quad (4)$$

The head-tail damping rates are given by

$$\frac{T_0}{\tau_x} = 0.56 \times 10^{-3} I(mA)\xi_x \quad (5)$$

$$\frac{T_0}{\tau_y} = 2.4 \times 10^{-3} I(mA)\xi_y. \quad (6)$$

At $I = 0.22 mA$/bunch and $(\xi_x, \xi_y) = (5, 8)$, the damping times are

$$\tau_x = 16 ms \quad (7)$$

$$\tau_y = 2.4 ms \quad (8)$$

2.4.2 LER

A measurement at a single bunch operation shows

$$\frac{d\nu_x}{dI} = -0.0015 mA^{-1} \quad (9)$$

$$\frac{d\nu_y}{dI} = -0.0034 mA^{-1} \quad (10)$$

The transverse wake forces are estimated to be

$$W_{1,x} = 0.63 \times 10^{18} z[V/Vm] \quad (11)$$

$$W_{1,y} = 1.4 \times 10^{18} z[V/Cm]. \quad (12)$$

The head-tail damping rates are given by

$$\frac{T_0}{\tau_x} = 0.84 \times 10^{-3} I(mA)\xi_x \quad (13)$$

$$\frac{T_0}{\tau_y} = 2.0 \times 10^{-3} I(mA)\xi_y. \quad (14)$$

At $I = 0.5mA$/bunch and $(\xi_x, \xi_y) = (5, 8)$, the damping times are

$$\tau_x = 4.8ms \quad (15)$$

$$\tau_y = 1.3ms \quad (16)$$

2.5 Vertical beam blow-up in LER

Vertical blow-up of beam size is observed in LER.

The beam size as a function of beam current starts to increase at a threshold beam current and is almost doubled by 300 mA under typical operating conditions.

The blow-up is one of the most serious problems limiting the luminosity of KEKB.

2.5.1 Characteristics of the beam blow-up observed by the interferometer

1. Single beam and multibunch effect.

2. The effect is confined in a train, if the separation between trains is sufficiently long (longer than about 160 buckets).

3. The blow-up has a threshold which is determined by the charge density (bunch current/bunch spacing).

4. The blow-up does not change much for the chromaticity.

5. Almost independent on betatron tunes.

6. No dependence on vacuum pressure (especially on hydrogen) in the arc.

7. No dependence on the position of the vertical masks.

8. No dependence on the excitation of the wigglers.

2.5.2 Beam size of each bunch

If the blow-up is caused by the electron cloud, we expect the beam size increases along the train because the density of the cloud also increases along the train.

1. Average beam size Beam size was measured by the interferometer by adding the bunch one by one to the train.

   The data shows that the average beam size increases as the length of the train increases.

2. Measurement by the Fast Gated Camera We are trying the direct measurement of the beam size by the fast gated camera.

   The data shows that the beam size increases along the train and the beam size almost saturates at 20th bunch.

2.5.3 Tune along the train

Vertical betatron tune of the bunches along the train was measured by the gated tune meter.

The data show that

1. tune increases along the train,
2. tune almost saturates at about 20th bunch,
3. tune shift is proportional to the charge density of the beam and (saturated tune shift) / (charge density) is about 0.12.

2.6 Permanent-magnets as photoelectron cleaner

To remove the electrons, about 5000 permanent magnets were attached on the outer-lateral side of the vacuum chambers where the synchrotron radiation irradiate.

The magnets are attached in every 10 cm of the LER drift space within 7 m downstream from bending magnets.

We tried two type of magnets , i.e. string type and C yoke type. At first string type magnets were tried. Then they were replaced with C yoke magnets because the blow-up still remained and a strange instability appeared around 20 mA.

The measurement by the interferometer showed slight improvement of the blow-up when the bunch spacing is larger than or equal to 8 rf buckets. But the effect was not remarkable.

Two hypotheses are proposed to explain why the magnets are not effective if the blow-up is caused by the electron cloud.

1. Reflective light hits the inner-lateral side of the chamber where the magnets are not attached and it generates the electrons.

2. High energy photoelectrons (several keV) ,which are not swept out by the magnetic field, are produced due to shallow incident angle.

To examine the hypotheses,

1. the measurement of the current through BPM electrodes are in progress and

2. the measurement of reflectivity of light and energy distribution of photoelectrons is planned at KEK PF.

3 Model and simulation

3.1 General

We simulate these phenomena by solving equations of motions of beam and electron/ion. These phenomena are governed by the same equation of motion. In a rigid bunch model, the motion of bunch ($\bar{\boldsymbol{x}}_e$) and cloud particles ($\boldsymbol{x}_{i,j}$) are expressed by

$$\frac{d^2\bar{\boldsymbol{x}}_e}{ds^2} + K(s)\bar{\boldsymbol{x}}_e = \frac{2r_e}{\gamma}\sum_{j=1}^{N_i}\boldsymbol{F}_G(\bar{\boldsymbol{x}}_e - \boldsymbol{x}_{i,j})\delta(s - s_e), \tag{17}$$

$$\frac{d^2\boldsymbol{x}_{i,j}}{dt^2} = \frac{2N_e r_e c^2}{M_i/m_e}\boldsymbol{F}_G(\boldsymbol{x}_{i,j} - \bar{\boldsymbol{x}}_e)\delta(s_i - s_e), \tag{18}$$

where $\boldsymbol{F}_G$ is expressed by Bassetti-Erskine formula,

$$F_{G,y}(\boldsymbol{x}) + iF_{G,x}(\boldsymbol{x}) = \sqrt{\frac{\pi}{2(\sigma_x^2 - \sigma_y^2)}} \tag{19}$$
$$\left[w\left(\frac{x+iy}{\sqrt{2(\sigma_x^2-\sigma_y^2)}}\right) - \exp\left(-\frac{x^2}{2\sigma_x^2} - \frac{y^2}{2\sigma_y^2}\right) w\left(\frac{\frac{\sigma_y}{\sigma_x}x + i\frac{\sigma_x}{\sigma_y}y}{\sqrt{2(\sigma_x^2-\sigma_y^2)}}\right)\right].$$

Asymptotic behavior

$$F_y + iF_x \implies \frac{y+ix}{r^2} \qquad x, y \to \infty$$

$$F_y + iF_x \implies \frac{1}{\sigma_x + \sigma_y}\left(\frac{y}{\sigma_y} + i\frac{x}{\sigma_x}\right) \qquad x, y \to 0$$

These instabilities

- Ion instability in HER.
- Photoelectron instability in LER : multi-bunch mode.
- Photoelectron instability in LER : single-bunch mode.

are similar (or equivalent) to

TWO STREAM INSTABILITY

studied in plasma physics.

Differenece of three instabilities

- Mass (ion and electron).
- Density of cloud.
- Frequency range (bunch by bunch and inner bunch correlations).

3.2 Ion instability in HER

Ions are produced by ionization of the residual gas in the beam chamber due to interaction with beam.

3.2.1 Mass

We consider $CO(A = 28)$ ion.

$$M_i/m_e = 53000 \tag{20}$$

3.2.2 Density of ion cloud

Production rate: $100m^{-1}$ by a bunch passage ($N_b = 1.4 \times 10^{10}$/bunch) at $P(CO) = 1nTorr$.

If they are accumulated by 100 bunches $n_{ion} = 10^4 m^{-1}$, neutralization factor ($2ns$ spacing) is

$$n_{ion}/n_b = 5 \times 10^{-7} \tag{21}$$

Ions are created near beam, their density is not small. Volume density near beam ($\sigma_x \times \sigma_y = 0.4 \times 0.06mm^2$)

$$\rho_{ion} = 1 \times 10^{11} m^{-3} \tag{22}$$

3.2.3 Frequency

If $\boldsymbol{x}_b = 0$, ions oscillate in linearized force (trapping) by a series of bunches,

$$\omega_i^2 = \frac{2n_e r_e c^2}{M_i/m_e} \frac{1}{\sigma_y(\sigma_x + \sigma_y)}, \tag{23}$$

Considering coherent motion of rigid bunch and rigid ion

$$\sigma \to \Sigma = \sqrt{\sigma_{ion}^2 + \sigma_{beam}^2} \tag{24}$$

At $N_b = 1.4 \times 10^{10}$/bunch and $\sigma_x \times \sigma_y = 0.4 \times 0.06 mm^2$,

$$2\pi/\omega_i = 65ns \quad \text{2ns bunch spacing} \tag{25}$$

$$= 91ns \quad \text{4ns} \tag{26}$$

$$= 130ns \quad \text{8ns} \tag{27}$$

Beam is modulated in transverse direction by the ion frequency. A dipole mode of bunch by bunch correlation (coupled bunch instability) occurs.

3.2.4 Simulation results

Simulation results obtained by solving equations of motion.

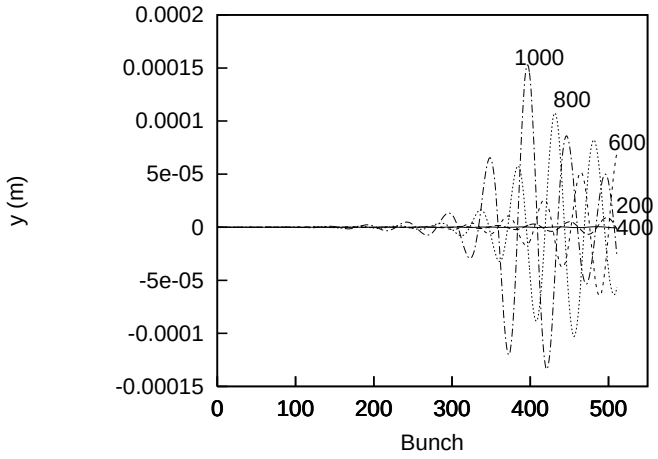

Figure 1: Coupled-bunch pattern due to the fast ion instability. The vacuum pressure is assumed to be 1 nTorr. Bunch patterns at the 200, 400, 600, 800, and 1000-th revolution are drawn.

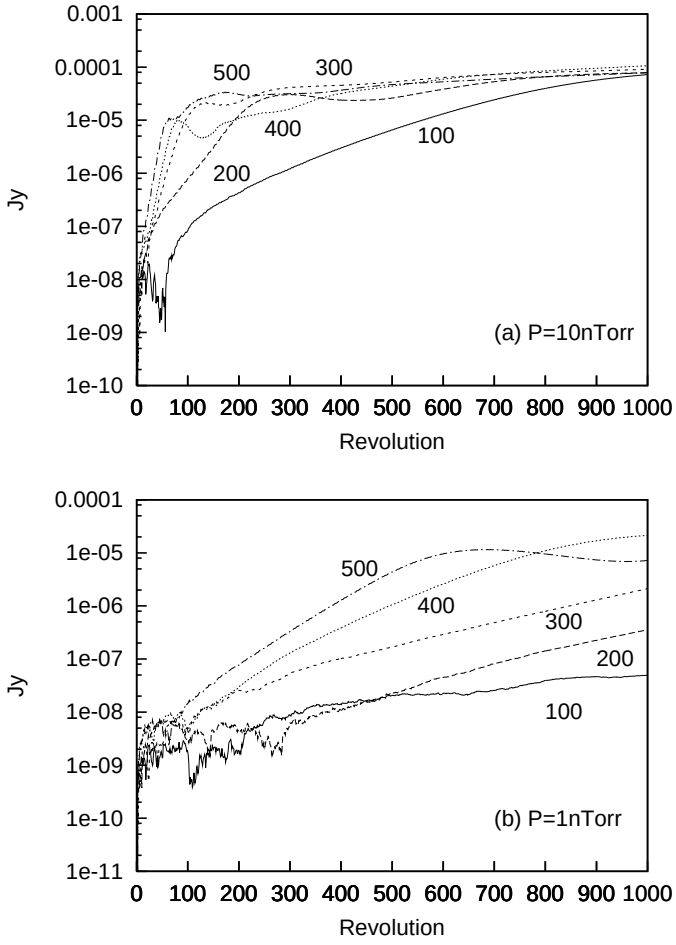

Figure 2: Time evolution of the amplitude of each bunch amplitude. Amplitudes of 100, 200, 300, 400, and 500-th bunches are plotted for $P = 10^{-8} Torr$ (a) and $P = 10^{-9} Torr$ (b).

3.3 Photoelectron instability in LER : Multi-bunch mode

3.3.1 Density of electron cloud

Photoelectrons are produced due to that synchrotron radiation of beam hits the chamber wall. The quantum efficiency for incident photon and energy distribution of photoelectrons are considered 0.1 and several eV.

$5 \times 10^8 e^-/m$ are produced by a bunch passage ($N_b = 3.3 \times 10^{10}$/bunch) at the chamber wall.

Equilibrium denisity of electron cloud is estimated by solving the equation of electrons for $\boldsymbol{x}_b = 0$. Here electrons are created by every passage of bunches.

$$\frac{d^2\boldsymbol{x}_{e,j}}{dt^2} = 2N_e r_e c^2 \boldsymbol{F}_G(\boldsymbol{x}_{e,j} - \bar{\boldsymbol{x}}_b), \tag{28}$$

We assume that photon reflection rate is 0.3 and secondary electrons are produced for incident electron energy threshold of $E_{th} = 150eV$. The number comes up to near neutralization level.

$$n_e/n_b \sim 0.4 \qquad n_e \sim 2.4 \times 10^{10}/m \tag{29}$$

$$n_e/n_b \sim 0.5 \qquad n_e \sim 0.7 \times 10^{10}/m \tag{30}$$

The volume density near beam is also estimated by

the simulation

$$\rho_e = 8 \times 10^{12} m^{-3} \quad \text{2ns bunch spacing} \tag{31}$$

$$\rho_e = 0.7 \times 10^{12} m^{-3} \quad \text{8ns} \tag{32}$$

3.3.2 Frequency range

Since electrons are not trapped by a series of bunches, there is no characteristic frequency like ion trapping.

Electrons absorbed to the chamber wall after one or a few approach to beam, that is, they stay in the beam chamber during several 10 to 100 ns. Range of bunch by bunch correlation is also several 10 to 100 ns.

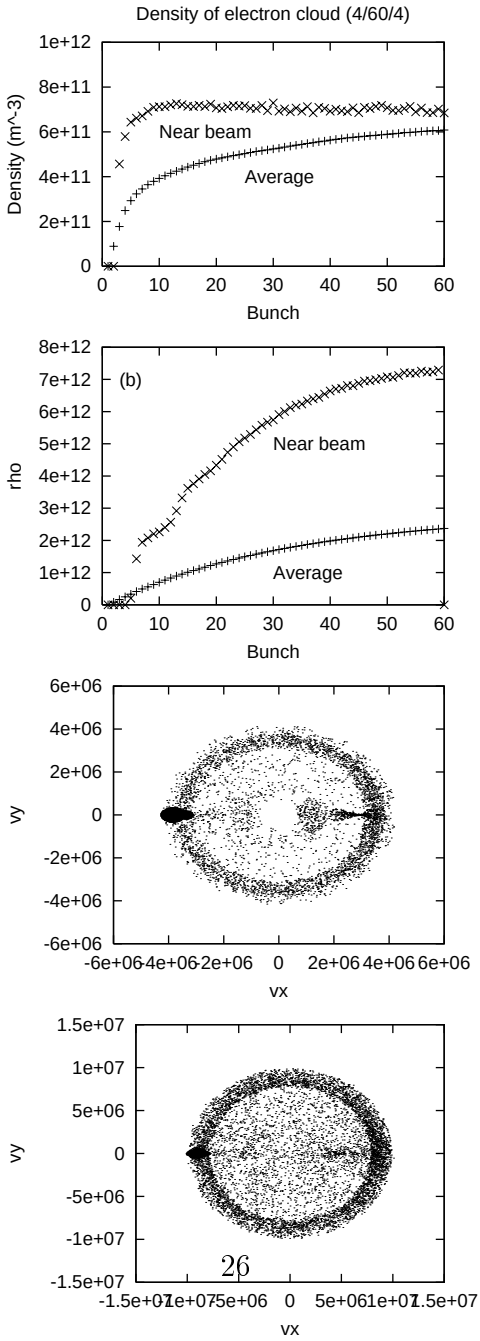

Figure 3: Density and velocity distributions of electron cloud. (a) and (b) are electron densities for $8ns$ and $2ns$ spacing, respectively. The cross and diamond correspond to averaged density and local one near beam, respectively. (c) and (d) are velocity distributions for $8ns$ and $2ns$ spacing, respectively.

3.3.3 Simulation

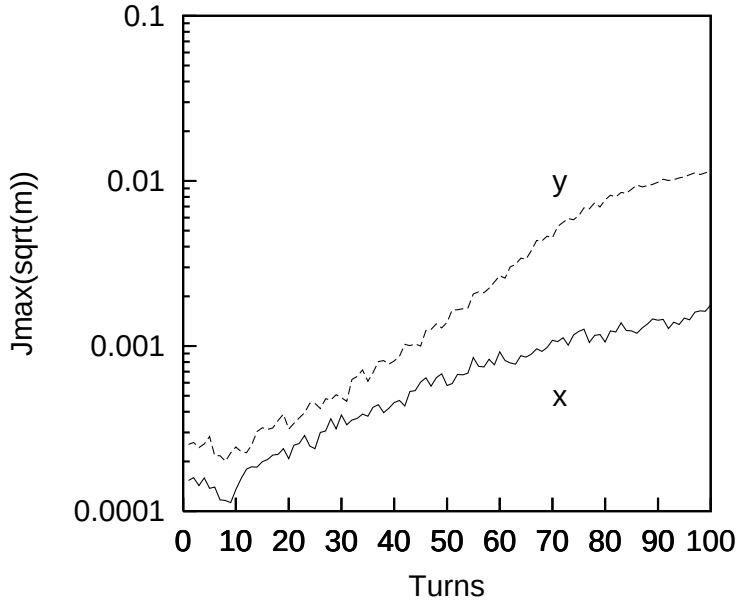

Figure 4: Amplitude growth obtained by tracking.

The growth rates are about $0.03(0.3ms)$ in horizontal and $0.07(0.15ms)$ in vertical at $I = 2.6A$ filling every buckets.

At $I = 500mA$ filling every 4 buckets, the growth is guessed about a few ms.

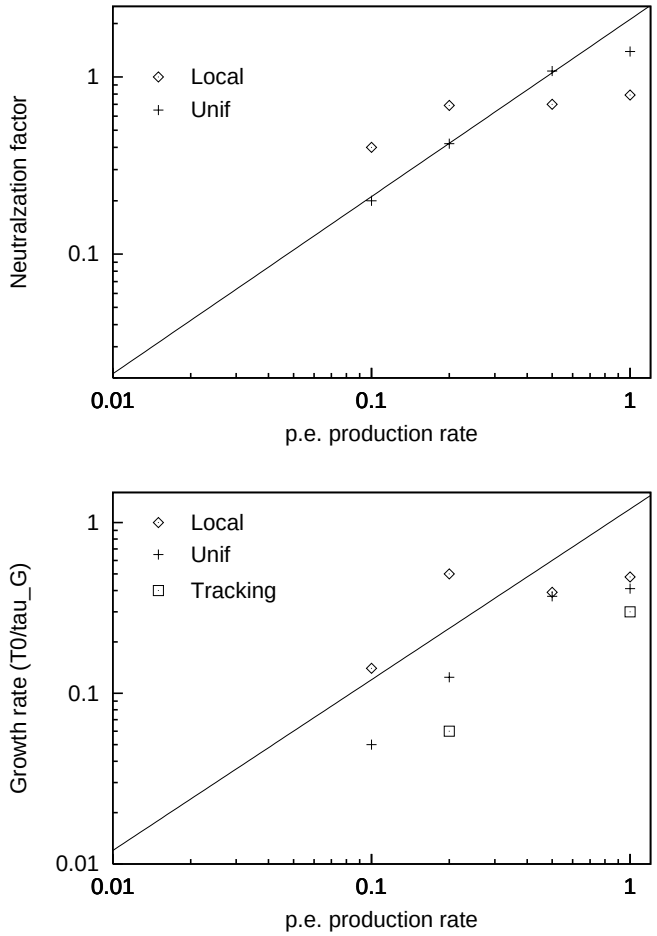

Figure 5: Neutralization factor and growth rate for various photoelectron production efficiency.

3.4 Photoelectron instability in LER : Single-bunch mode

3.4.1 Density of electron cloud

Density of electron cloud was obtained before (Sec.3.3),

$$\rho_e \sim 10^{12} m^{-3} \tag{33}$$

Tune shifts is caused by the electron cloud

$$\Delta\nu_y = \frac{r_e}{\gamma} < \beta_y > \rho L \qquad \text{Planer} \tag{34}$$

$$= \frac{r_e}{2\gamma} < \beta_y > \rho L \qquad \text{Cylindrical} \tag{35}$$

At $\rho = 10^{12} m^{-3}$

$$\Delta\nu_y = 0.012 \qquad \text{Planer}$$

$$\Delta\nu_y = 0.006 \qquad \text{Cylindrical.}$$

3.4.2 Frequency

Electrons oscillate in an electric potential of a positron bunch.

$$\omega_e^2 = \frac{2n_e r_e c^2}{\sigma_y(\sigma_x + \sigma_y)}, \tag{36}$$

where $n_e(m^{-1})$ is charge density in a positron bunch. Considering coherent motion of rigid bunch and rigid cloud

$$\sigma \to \Sigma = \sqrt{\sigma_{ion}^2 + \sigma_{beam}^2} \tag{37}$$

At $N_b = 3.3 \times 10^{10}$/bunch, $sigma_z = 4mm$ and $\sigma_x \times \sigma_y = 0.4 \times 0.06mm^2$,

$$n_e = 4 \times 10^{12} m^{-1} \tag{38}$$

$$\omega_e = 2\pi \times 45GHz \tag{39}$$

3.4.3 Head-tail instability due to electron cloud

Bunch is modulated in transverse direction by the electron frequency. If there is no synchrotron oscillation like LINAC, beam breakup (BBU) occurs. In storage rings, positrons in a bunch oscillate in longitudinal phase space with a synchrotron tune. The BBU transforms into head-tail instability.

3.4.4 Simulation results

A positron bunch is represented by micro-bunches with the same transverse size as that of the bunch. The micro-bunches are distributed in longitudinal phase space. We solve equation of motion of positron micro-bunches and electrons.

These figures show a bunch shape in $z - p_z - y$ space. Multi air-bag model is used for the longitudinal distribution to visualize.

Excitation of the head-tail motion ($m = -1$) means a beam size blow up. This phenomenon may explain the beam blow up in LER.

4 Summary

We discussed the instabilities observed in KEKB.

- Coupled bunch instability in HER
- Coupled bunch instability in LER
- Beam size blow up in LER

We have performed simulations for

- Coupled bunch instability due to ion cloud
- Coupled bunch instability due to photoelectron cloud
- Head-tail instability due to photoelectron cloud.

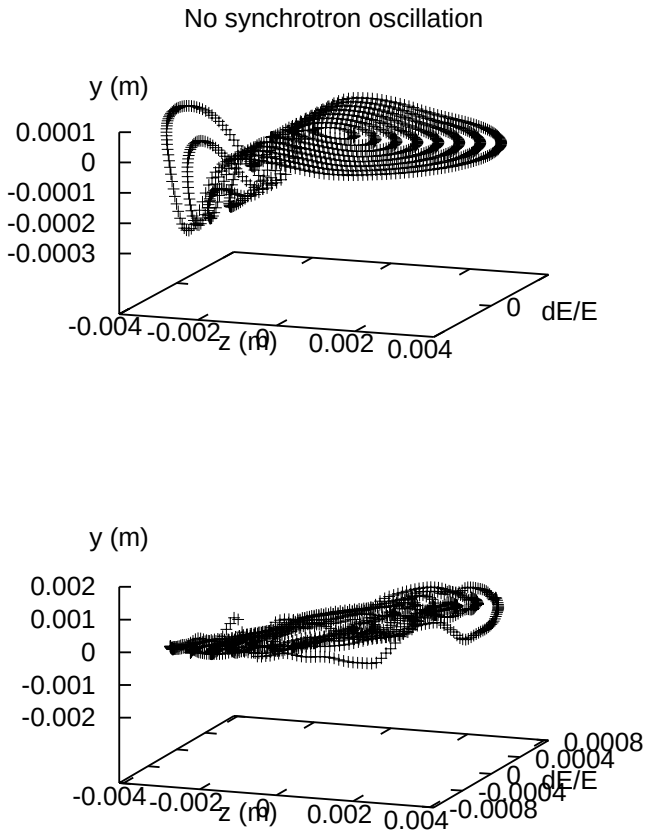

Figure 6: Bunch shape without/with syncrotron oscillation. ($\nu_s = 0.015$)

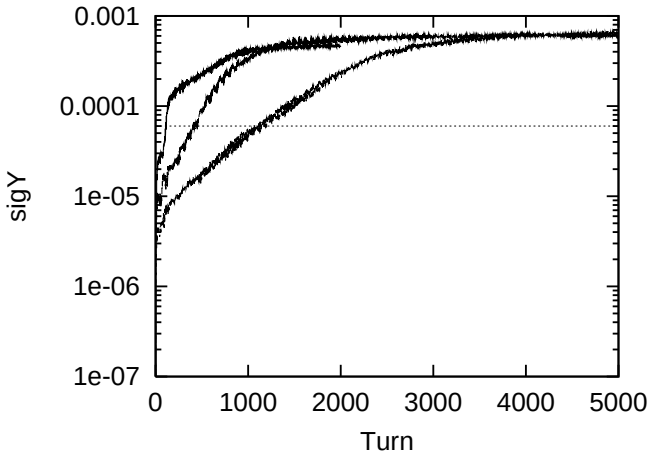

Figure 7: Growth of vertical beam size. Densities of electron cloud are 2×10^{11}, 4×10^{11}, and $7 \times 10^{11} m^{-3}$.

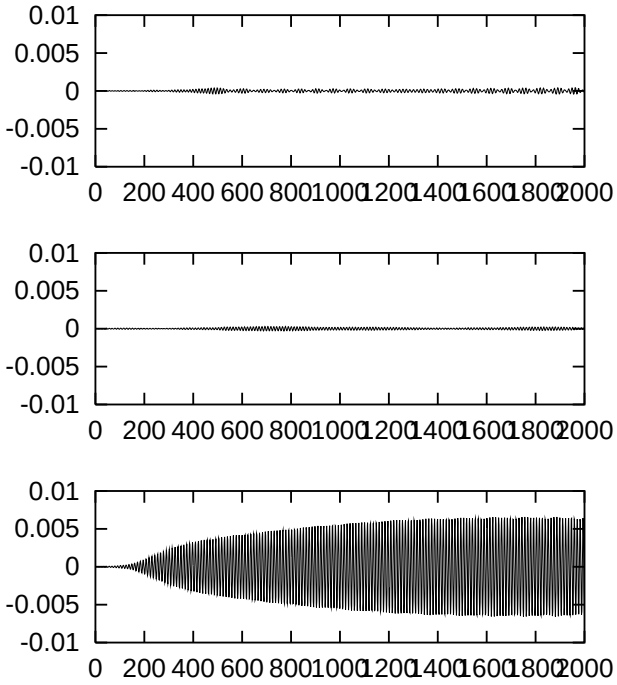

Figure 8: Dipole mode ($\xi = 8$,0, and -8).

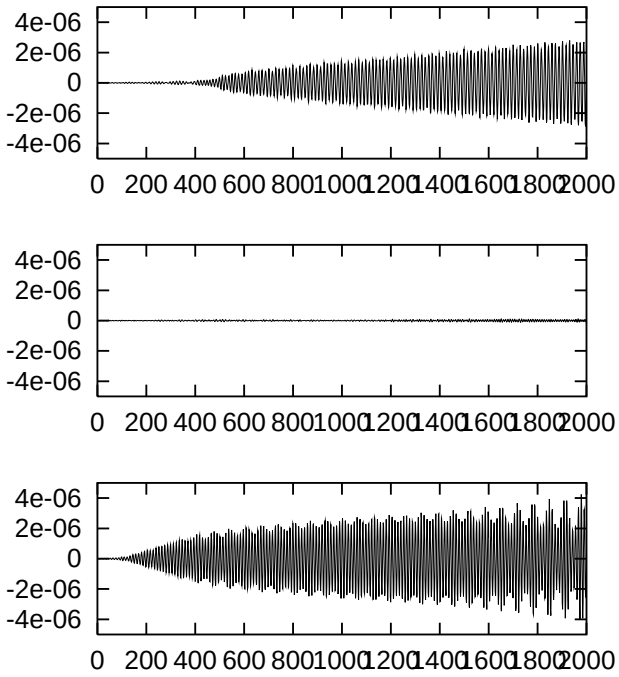

Figure 9: $< yz >$ ($\xi = 8$,0, and -8).

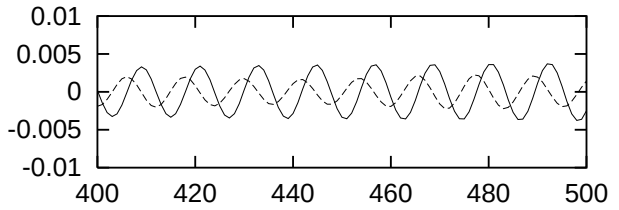

Figure 10: Correlation of $\langle y \rangle$ and $5\langle yz \rangle / \sigma_z$ ($\xi = -8$).

The simulations seem to be consistent with the experiments. Ion instability is expected to be reduced by improvement of vacuum pressure. If the instability in LER is due to photoelectron cloud, we have to take drastic measure to improve. There is no definitive evidence to identify the instability yet, though there are many consistent results.

LER current is limited by heating of hardware especially moving masks and a bellows near IP. The masks seem to be heat up due to HOM. Impedance of moving mask is source of a longitudinal instability.

Challenge to higher current and machine studies are continued after improvement of the masks at March. We expect to go forward.